

A passive receiver for exploiting high-frequency broadband acoustic emitters for improved situational awareness

Abstract — Over the past twenty years, a large and growing number of high frequency active sonars have been developed for military, commercial and recreational use. These systems are increasingly used by surface and submerged platforms for underwater communication, underwater navigation, bathymetry, fish finding, bottom imaging, fishing net monitoring, obstacle and terrain avoidance, and many other tasks. In the past, these systems relied on pulsed CW, but recent cost reductions in sensor and processing electronics have resulted in a transition to higher performance systems employing FM sweeps providing better range resolution and low Doppler performance. Commercial and recreational broadband sonar variants are becoming commonplace on boats of all sizes with complete high frequency systems using broadband ‘chirp’ technology now available for as little as a few hundred dollars. The new frontier in high performance are active emitters using Direct Sequence or Frequency Hopping Spread Spectrum (DSSS or FHSS) waveforms or pseudorandom noise (PN) waveforms to provide even better range resolution and low Doppler performance. These waveforms require significantly more processing than FM but as this becomes less expensive, more systems will undoubtedly transition.

Many common emitters are not being detected by legacy wideband receivers due to their high frequencies, their broadband waveforms, or both. Wideband directional sensors with increased bandwidth and broadband processing can be used to counter-detect these emitters at significant ranges improving situational awareness using small, low-cost, low-power, passive broadband receivers which can be deployed on manned or unmanned platforms. With appropriate post-detection software, emitter’s can be localized and tracked, and in some cases classified based on the received waveform.

Sweden has been an early leader in incorporating wideband acoustic receivers onto their submarines because the Baltic is so noisy at traditional sonar frequencies. In consultation with Swedish technical experts, the author designed a 512 kHz system for the Gotland Class Submarines twenty years ago. Since then, the frequency band which should be covered has expanded and increasingly common use of broadband and even spread spectrum signals requires more sophisticated sensors, electronics, and processing. At the same time, the desire to use these sensors on UUVs makes good SWaP characteristics essential and emphasizes the need to reduce the costs associated with manufacturing, installing, testing and maintaining these sensors.

A small (13 x 24 x 2cm), directional, low-cost (\$20K), low-power (5W), hydrodynamic, seven-element wideband (1 to 625 kHz) receiver in a blade shape has recently been developed to detect and localize high-frequency broadband emitters. The receiver provides close to 4π steradian coverage, is powered and communicates via a single SubConn 13-wire power and Gb Ethernet cable, has simple installation requirements and can improve situational awareness of surface vessels, UUVs and submarines. This paper describes issues associated with developing this type of sensor and provides early tank testing results.

1 Objective and Benefits

Wideband passive receivers with broadband detectors provide increased situational awareness by facilitating counter-detection, localization and tracking of increasingly common high frequency, broadband acoustic emitters that many currently fielded receivers are unable to detect because they have limited frequency range, lack broadband detection capability, or both. Wideband passive receivers are small and not inherently expensive, but they are not commonly used on platforms because data rates and processing requirements are high and because there is insufficient awareness of the ability to counter-detect high frequency broadband signals at considerable ranges.

At this point in time it has become possible to integrate low-cost, directional, wideband sensors with FPGA based broadband processing to allow near-optimal counter-detection of common high frequency broadband emitters at significant ranges. This paper discusses the development of a wideband device with a broadband detection capability along with technical and programmatic challenges and potential solutions to these challenges.

2 Introduction

2.1 Waveform Evolution

Thirty years ago, most sonar systems made use of pulsed CW waveforms, i.e. waveforms with a BT (Bandwidth-Time) product of unity, at fixed frequencies. These sonars could be effectively counter-detected by platforms using spectral analysis based narrowband receivers with sufficient bandwidth. The advent of the FFT allowed this processing to be performed very efficiently and the detectors on many early counter-detection sonars were based on repurposed spectrum analysers. Near optimal performance was possible with a few FFT lengths followed by a few post-detection integration periods.

At that time, FM waveforms were employed mainly by military sonars for detecting low range rate threats. Early military FM sonars generally had BT products of around 75 and many considered the DICASS FM waveform’s BT product of 400 to be excessive. But twenty years ago as better electronics for processing and modulation and demodulation became available, sonar systems began transitioning to more widespread use of FM waveforms, in many cases with larger BT products of up to 1000.

The desire to efficiently counter-detect these FM pulses presented problems for system designers. The obvious solution when using spectral analysis, i.e. integrating over the FM pulse’s entire BT space, provides very poor counter-detection performance with degradation increasing with the BT product. This was unacceptable, so these waveforms were generally counter-detected either by approximating a tracking filter by piecing together shorter,

more narrowband pieces of the FM pulse, or in some cases an FM demodulator with a fast lock-on time was added to search for FM signals. Neither solution is near optimal.

About twenty years ago, commercial and recreational sonars began transitioning to wideband FM sweeps. These systems, marketed as ‘chirp’ technology, provide greater range resolution and better ability to detect low Doppler targets (usually fish) close to an extended target (usually the bottom). These systems use FM sweeps with bandwidths of 20 to 320 kHz and TB products between 100 and 1000. Military sonars using high-frequency fast FM sweeps also began to be commonly used for obstacle and terrain avoidance and for harbour defence.

At about the same time, a few systems were developed which made use of spread spectrum techniques to generate broadband signals without narrowband components and with thumbtack ambiguity functions providing simultaneous range and Doppler information. The drawbacks with using these waveforms are the required low-Q, wideband projectors and a need for much more receive processing than FM sweeps. Unlike FM sweeps, spread spectrum cannot be detected by piecing together short, narrowband segments, so these waveforms are frequently claimed to be LPI (Low Probability of Intercept). These signals may be nearly impossible to detect using a narrowband detector but can be nearly optimally detected using a broadband detector.

A good spread spectrum example is L3 MariPro’s HAIL acoustic modem [1] which uses DSSS (Direct Sequence Spread Spectrum) for data communication while simultaneously providing range and range rate between the transmitter and receiver. The white spectrum of its ~8 kHz BW signal prior to being filtered by the projector is shown in figure 1 below. The performance of a narrowband detector against this type of spread spectrum signal will be very poor, even with perfect knowledge of the signal bandwidth and on/off times, but a good broadband receiver with a priori knowledge of the frequency band can detect this signal about as well as the HAIL receiver itself.

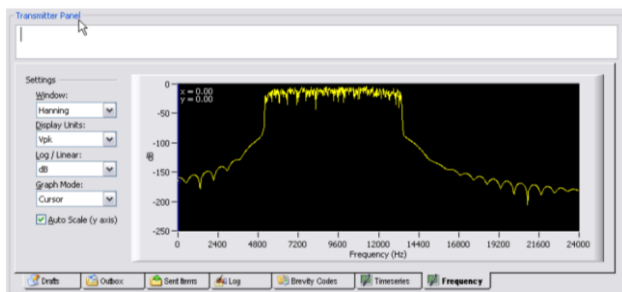


Fig. 1. L3 MariPro’s HAIL acoustic modem’s DSSS spectrum prior to projection. This broadband signal won’t be detected by narrowband detectors and is described by the manufacturer as LPI, but a GCC based broadband detector will detect it at about the same range as the modem’s detector which uses replica correlation based on the originally transmitted waveform. This system can be used to determine a platform’s broadband detection capability in the HAIL system’s frequency band.

Today, even higher performance spread spectrum systems are beginning to appear for commercial use and should become more widely available as the cost of processing hardware continues to decrease. Spread

spectrum systems for the more price sensitive recreational market are still a few years away, but they’re coming.

Despite the poor counter-detection performance of spectral analysis based narrowband detectors against high BT product FM waveforms and extremely poor performance against spread spectrum waveforms, most fielded passive receivers still rely on narrowband detectors to counter-detect these increasingly common broadband emitters.

2.2 Frequency coverage

Another serious drawback of many passive counter-detection receivers is failure to cover the frequency band where most sonar systems operate. While most new sonar systems are using frequencies well above 100 kHz, most wideband receivers are limited to roughly 100 kHz and many technical issues arise when trying to build receivers that cover an extended frequency range, especially when using a single hydrophone to cover the entire frequency range. The problem is that a smaller hydrophone required to get an omni pattern with a high enough resonant frequency will have poor sensitivity, and this low sensitivity increases the difficulty of keeping electronic self-noise well below ambient noise.

The best performing method of solving this problem is to use multiple sets of hydrophones to cover the band. 40 kHz is a reasonable break frequency allowing use of larger, more sensitive phones to cover the important upper mid frequency range where ambient noise is low during low sea states as shown in figure 3. An inexpensive hydrophone such as the Calibrated Omni used in DIFAR and VLAD sonobuoys makes a fine choice. Figure 2 below shows an four hydrophone A-size sensor built by USSI developed for the Liquid Robotics WaveGlider.



Fig. 2. An A-size receive array built by USSI using Calibrated Omni sensors for mammal detection using the Liquid Robotics WaveGlider towfish.

Using multiple sets of phones has the downside of significantly increasing size and complexity of the system, making the system more expensive as well as harder to install, especially on smaller platforms.

Another issue with a wider frequency band is that faster A/D converters are required. For best performance these converters must have the highest possible dynamic range, but A/D dynamic range decreases with sample rate. The best A/D converters for sampling at 1.5MHz currently provide 18 to 18-1/2 bits of dynamic range. A/D convert clock jitter also becomes a more significant noise

generator at higher frequencies and must be taken into consideration at frequencies above 400kHz or so.

Another issue is that to provide good directional coverage over a wide frequency band, the phones must be placed in locations which result in the array being sparse over most of the band. The Blade Sensor's phones are spaced 1.5" (3.81cm) apart which means $\frac{1}{2}$ lambda spacing occurs at about 19 kHz. Luckily almost all high frequency signals of interest are broadband in nature, so this isn't as much of a problem as one might expect.

A final issue is the data rate from the wideband sensor. At the Blade Sensor's sample frequency of 1.25MHz, the seven channels generate 210Mb of raw data per second. This is a comfortable fit for Gb Ethernet, but it is a lot of data to store and to process.

3 System design

3.1 System considerations

Constructing a sensor that is small, low-cost, low-power, widely applicable, and can cover a wide frequency band with integrated broadband processing is a non-trivial task. To ensure the sensor meets these requirements, the development was focused on compatibility with the small UUV market, typified by the Hydroid Remus 100 [2]. These UUVs are frequently outfitted with RDI's DVL type devices in an A-size housing and our goal was to have less platform impact than RDI's sensor. The desired sensor metrics used in the design of the sensor hardware are given in table 1 below:

Table 1. Desired wideband sensor metrics.

- Frequency coverage 1 to 625 kHz
- Spatial coverage Close to 4π steradian
- Counter detection ratio >2.5 times
- Signal clipping level >180dB re $1\mu\text{Pa}$ per $\sqrt{\text{Hz}}$
- Electronic noise level <30dB re $1\mu\text{Pa}$ per $\sqrt{\text{Hz}}$
- RMS bearing error < 3° @ MDL+15dB at boresight
- Dynamic range >120dB 1 tone, 100dB 2 tone
- Cable I/F 13-pin power + Gb Ethernet
- Power <5W
- Cost <\$20K

The first decision when designing a new array is the spatial distribution of the hydrophones. In an ideal world, a volumetric array would be implemented to simultaneously maximize directivity and coverage, but there are two major drawbacks to this approach. First, potting materials tend to be lossy at high frequencies, so a volumetric array that requires acoustic ray paths of significant length through the potting material tend to work poorly. Free-flooding the array is an option, but this requires an outer shell which means an additional surface where lensing will take place. A second issue is reflections off nearby structure which is generally problematic with volumetric arrays since they require a volumetric structure to hold the elements. Planar arrays can avoid these two problems by using a thin layer of potting material and avoiding potentially reflective surfaces near the array. A planar array was selected for the blade sensor for these

reasons and also because this shape allows construction of a hydrodynamic array without giving up spatial coverage. Each of the hydrophones in the planar array is mounted to allow visibility to both sides of the structure. This approach has the advantages of providing full spatial coverage and significantly reduces issues with reflections but has the disadvantages of left/right ambiguity and converting sound speed errors into AoA errors. These disadvantages will be resolved in an upcoming modification which will add a small volumetric array component to the sensor using an eighth hydrophone.

The blade sensor uses a single set of seven $\frac{1}{2}$ cm spherical air-backed hydrophones to cover the entire band. These phones have a resonant frequency of about 370 kHz, a sensitivity of $-213 \pm 2\frac{1}{2}$ dB and a capacitance of 1.8nF. We wish these numbers were higher, especially the

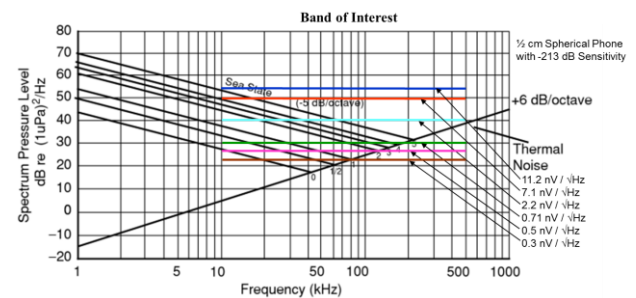


Fig. 3. Preamp RTI (Relative to Input) noise floor for a system with -213 dB re $1\mu\text{Pa}$ per $\sqrt{\text{Hz}}$ sensitivity hydrophones. Preamp noise floor is really important for this system!

resonant frequency which limits the top-end of the band.

The preamp is a critical part of any wideband sensor and preamp improvements are generally the easiest and most cost-effective method for improving system performance. The Blade Sensor's preamp-digitizer has an electronic RTI (Relative to Input) noise floor of 0.7nV per $\sqrt{\text{Hz}}$. In conjunction with the hydrophone's -213 dB sensitivity, this provides an equivalent electronic noise floor of 30 dB re $1\mu\text{Pa}$ per $\sqrt{\text{Hz}}$ as shown in figure 3 below.

In conjunction with the hydrophones, the preamp's RTI (Relative to Input) noise floor establishes the sensor's self-noise floor. The sensor noise floor for the hydrophone described above is shown in figure 3 operating with preamps ranging from a very low RTI noise level of 0.3nV per $\sqrt{\text{Hz}}$ to a very high RTI noise level of 11.2nV per $\sqrt{\text{Hz}}$. It can be seen that even the quietest preamp will significantly raise the sensor's noise floor at low sea states, while the noisiest preamp raises the noise floor of the entire band by up to 35 dB. In low sea-state conditions electronic self-noise level establishes the system's noise floor over a large portion of the spectrum, so consideration of methods to push this down further are justified. The preamp electronic noise floor is dominated by the contribution from two low-noise BF862 JFETs used as the hydrophone interface. The BF862 is a good choice as shown in figure 4 below. Lower noise JFETs are available from InterFet, but these have much higher input

capacitance, which acts as a voltage divider with the capacitance of the hydrophone.

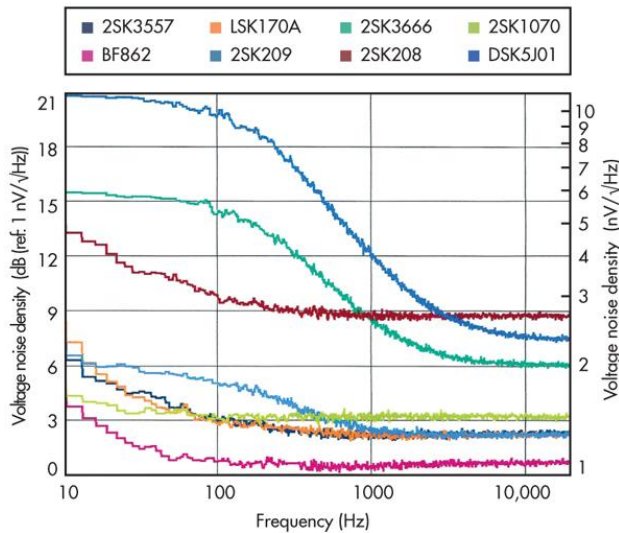


Fig. 4. All JFETs are not created equal. The no longer in production BF862 has considerably better noise characteristics than alternative low capacitance, low voltage JFETs. Measured data from Dimitri Danyuk, “Measurements Rate SMT Low-Voltage n-JFETs Under Consistent Conditions”, 19 April 2013.

The low frequency limit of the array is set by the array’s small aperture which leads to poor bearing accuracy and increased susceptibility to flow noise. Since this is inherently a high frequency array, a lower frequency limit above 5 kHz should be acceptable.

Another early decision was to use a COTS FPGA processor board mounted on the sensor PCB, rather than implementing the design directly on the PCB. This simplified the software and hardware development processes and will make it easier to substitute later versions of the processing hardware. At some point in the future the FPGA will be implemented directly on the sensor PCB to reduce power and volume.

The FPGA board has five primary requirements. First, it must accept mode configuration commands from the platform and provide sensor status to the platform. Second, it must generate the convert clock for the A/D converters and bring in high speed data from their SPI interfaces. Third, it must perform narrowband and broadband detection processing. Fourth, it must format processed and raw data for transmission to the platform. And fifth, it must provide the Gb Ethernet I/F to the platform.

3.2 Hardware development

The sensor hardware consists of the array structure, the hydrophones, a galvanically isolated DC/DC SMPS (Switched Mode Power Supply) to efficiently convert platform power for use by the blade sensor, a quiet 5V supply for powering the preamp and for the A/D reference, a 2.5V power supply for powering the A/D converter and I/O circuitry, seven low noise preamp-digitizers, a COTS FPGA card, a power and Gb Ethernet SubConn cable, a 13-pin connector and the sensor potting material.

A key early decision was to use PCB (Printed Circuit Board) material for the sensor structure. This provides

many advantages which include the ability to specify a rugged, planar array with arbitrary shape with high dimensional tolerance and selectable thickness which can be constructed at low-cost anywhere in the world while also allowing power supplies, preamps, processing and communications electronics to be integrated directly into the sensor structure. A four-layer PCB was specified to reduce electronic noise and to allow hydrophone traces to be routed on a shielded inner layer. Standard PCB 1.6mm thick FR-4 material was selected to minimize cost.

The PCB structure was designed using KiCad 4.0.7 CAE software and 6 four-layer boards were constructed, but only two of these were fully populated. Four-layer boards were used to allow better noise shielding of the hydrophone lines and the preamps. Red solder mask and ENIG (Electroless Nickel Immersion Gold) coating on exposed pads were used to ensure the unit looks good with a clear potting material.

The ½ cm air-backed spherical hydrophones, one is shown in figure 5 below, were provided by Sensor Technology Ltd. These phones are resonant at approximately 370 kHz with -213dB re 1µPa per √Hz receive sensitivity and a capacitance of 1.8nF. Air backed spherical hydrophones offer the best performance for this type of application, but the cost of these phones drives the cost of the sensor. Lower cost hydrophones can be used, but performance will suffer due to lower sensitivity for other types of phones with the same resonant frequency.



Fig. 5. A Sensor Technology Ltd ½ cm spherical phone mounted in the Blade Sensor’s FR-4 PCB structure. The phones offer outstanding performance over the wide frequency band.

A COTS Altera Cyclone V SoC FPGA card is used to clock and acquire data from the seven A/D converters associated with the seven preamp-digitizer modules, to process the data, to frame the data, and to send the data to the platform via Gb Ethernet. The A/D converters are clocked at 1.25 MHz and the 24-bit data is brought into the FPGA using a 100 MHz bit-clock. In addition to sending back raw and processed data, the Gb Ethernet port can be used to reconfigure the unit’s operational mode or even upload new software and firmware.

The populated, pre-potted blade sensor is shown in figure 6 below. The PCB boards were manufactured and the component were installed by MacroFab in Houston, Texas. The pre-potted sensor is shown with one ½cm

hydrophone installed along with seven preamp-digitizers. The COTS high-performance FPGA board, which is required to acquire high-speed SPI data, support broadband processing and provide Gb Ethernet communication with the host is not mounted but the mounting holes for its two forty pin connectors are shown.



Fig. 6. Pre-potted blade sensor with seven ½cm phones in a hexagonal configuration. Preamp-digitizer electronics, power supply and COTS FPGA board are mounted on the same PCB.

The preamp-digitizer module is shown in figure 7 below. The 24-bit digitizer is integrated with the output of the preamp to minimize noise pickup. The bounding box size has dimensions of 0.4” by 1.2” which equates to 1.02 by 3.05 cm. The dual parallel BF862 JFETs shown on the left interface to the hydrophone and provide initial low-noise current and voltage gain with very high input impedance. The LTC 6362 differential opamp provides band shaping and additional gain and also provides a low-impedance, high-speed interface to the LTC2380-24 A/D converter on the right. Sampling at 1.25 MHz, the preamp-digitizer consumes a total of 40mW most going to the A/D.

The seven preamp-digitizers feed data via independent SPI busses to a COTS Terasic DE10 Nano board shown in figure 8. This board was chosen to allow the unit to be constructed quickly and to provide a mature hardware and software development platform. Other advantages include support for Gb Ethernet, and the reference design materials, including schematics and BoM (parts list), which are readily available for download. It is also reasonably priced at \$130. On the downside, this board

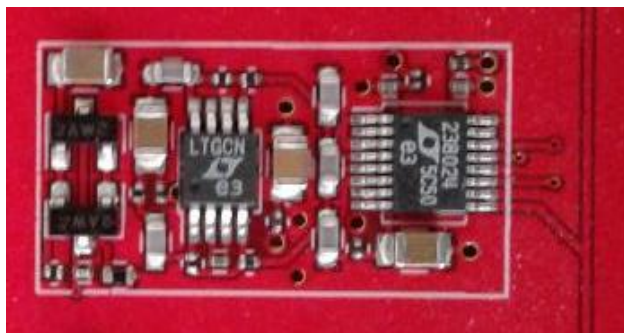


Fig. 7. One of the seven preamp-digitizer channels. The hydrophone input is on the left and the SPI bus interface, with convert and bit clock inputs and busy and serial data outputs, is on the right. 40mW is required, split between 2.5V and 5V rails.

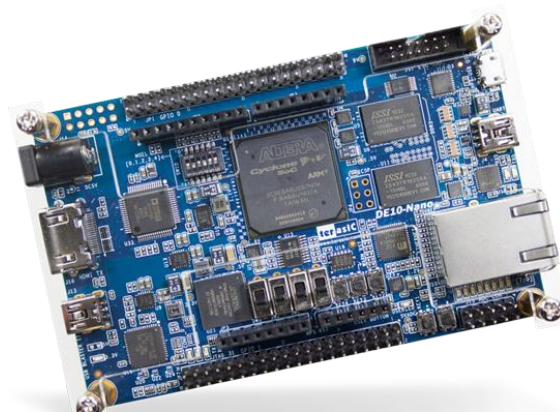


Fig. 8. The Blade Sensor uses the Terasic DE10 Nano Cyclone V SoC FPGA board for data acquisition, processing and I/O.

includes a lot of circuitry not required for the receiver, and its linear power supplies are not optimized for low power consumption.

In addition to providing the ½ cm spherical air-backed hydrophones, Sensor Technology Ltd also assembled and potted the prototype unit in black epoxy, as shown in figure 9 below. On the plus side, the potting looks good and imbues the unit with significantly greater structural integrity. On the minus side, many users prefer a transparent potting material to allow for visual inspections of the sensor internals, the potting material is rather thick, the potting material has absorption issues at high frequencies, and it has a significantly higher sound speed than seawater. Ideally, the potting material should have an acoustic impedance (ρc) between seawater and the PZT ceramic of the hydrophones, and a lower sound speed than seawater so that Snell’s Law bends the rays toward the planar array and not away from it.



Fig. 9. Epoxy potted blade sensor with planar array, electronics section at the base of the sensor, and 13-wire SubConn power and Ethernet cable which powers the sensor and provides Gb Ethernet communications between the sensor and the platform. The blade sensor is bracket mounted using four M6 bolts.

3.3 Processing

3.3.1 Signal conditioning

Processing begins with the hydrophone-preamp input signal conditioning. This is rarely emphasized, but in the case of a wideband receiver using a single hydrophone to cover the entire band, input signal conditioning is always a major performance driver. The LT SPICE preamp gain and phase curves for the Blade Sensor are shown in figure

10 below for the differential output that drives the digitizer (green), for the hydrophone input (cyan) and for the output of the JFET gain stage (red). Preamp gain from hydrophone to A/D converter input is a maximum of 40 dB which would provide a maximum 9.5 dBV signal at the A/D's 10V peak-to-peak input for a 180 dB re 1 μ Pa per $\sqrt{\text{Hz}}$ signal in the water with -213dB sensitivity hydrophone with 2.5dB hydrophone gain variation plus 40dB of preamp gain.

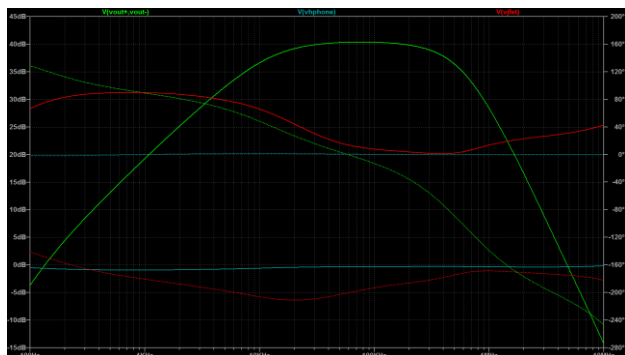


Fig. 10. Gain and phase curves for the preamp (green), the JFET output (red) and for the hydrophone input (cyan).

LT SPICE curves for preamp RTO (Relative to Output) noise are given in figure 11 below, with total noise (green), JFET noise (red), bias resistor noise (blue), drain resistor noise in cyan and opamp feedback resistor noise in magenta. As can be seen, the preamp noise is dominated by the JFET noise throughout the band, which is the desired result. RTI noise is obtained by dividing the RTO noise values by the gain relative to the hydrophone shown in figure 10 at the corresponding frequency.

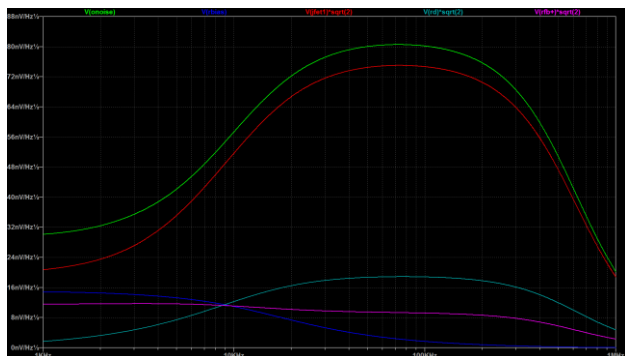


Fig. 11. LT SPICE noise simulation of the hydrophone input and the JFET output with a 25mV 25 kHz hydrophone signal.

An LT SPICE simulation of the response of the system when driven by a hydrophone at 25 kHz is shown in figure 12. The hydrophone input is shown in cyan while the single ended JFET output is shown in red and the preamp output, which is also the A/D input, is shown in green. The large transients on the preamp output are caused by the switched capacitors in the A/D converter's successive approximation circuitry. The preamp must be designed to quickly recover from these transients prior to the start of the next sampling period 800ns later.

Spectral analysis of the LT SPICE hydrophone input and JFET output are shown in figure 13 with the hydrophone (cyan) producing a 50mV peak-to-peak input signal. Self-noise on the hydrophone input signal is due to

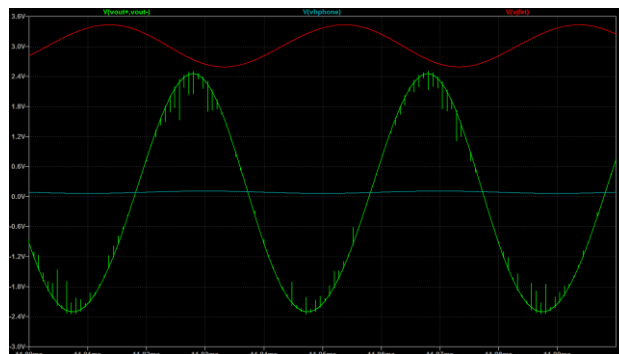


Fig. 12. LT SPICE transient simulation of the hydrophone input (cyan), the JFET output (red) and the differential preamp output (green) for a 25mV 25 kHz signal. The preamp output shows impulses from switching capacitors used for A/D conversion.

the bias resistor and leakage current from the JFET gates. The JFET output (red) show high dynamic range and 1/f noise below 10 kHz. The noise peak at about 10 kHz is from the 5V linear power supply. Even harmonics of the signal are not significant, and the third harmonic is down 30dB and the fifth harmonic is down 65dB. The high frequency noise above 1 MHz is due to the A/D's switched capacitance sampling transients and harmonics feeding back into the preamp signal path. This feedback is a significant noise contributor and ferrite chips are used between the differential opamp and the A/D converter prior to the capacitors to attenuate these transients.

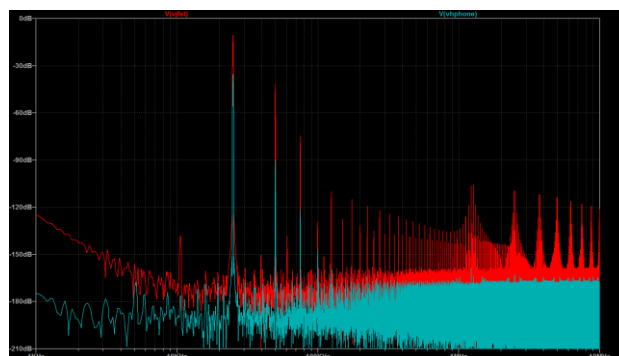


Fig. 13. RTO (Relative to Output) noise per root Hz for the preamp (green), the JFETs (red), the bias resistor (blue), the drain resistor (cyan) and the feedback resistors (magenta). Having the JFETs as the dominant noise source is desired behavior and indicates that performance can probably be improved by use of more JFETs in parallel.

3.3.1 Detection processing

Back when most signals were pulsed CW, detectors for passive intercept receivers could be much simpler. A few different overlapped, windowed FFT sizes would cover the range of pulse lengths which might include values such as 125 μ s, 1ms, 8ms, 64ms and 512ms. Post Detection Integration (PDI) would be used to provide a better match to pulse lengths between these values or longer than the longest FFT. Phase shift beamforming can also be implemented if the processing bandwidth allows. This processing, shown in figure 14 below, is both simple and

efficient. Things get only slightly more complicated when bins from successive FFTs are being stitched together to detect FM pulses. This type of detector was used in the processing for the Dutch Walrus Class submarines' passive intercept receiver.

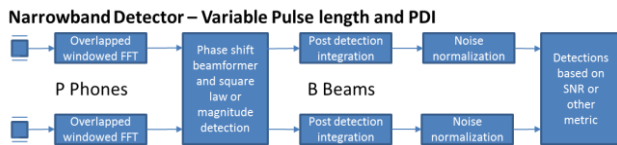


Fig. 14. High-level narrowband detection processing string.

Broadband processing, shown in figure 15 below has many more degrees of freedom including selection of frequency bands and pulse durations. Additionally, a transform filter can be applied to change the detection characteristics. The FFT length is not as critical and will be chosen to be short enough allow use of Welch's Method to integrate over time to search for varying pulse lengths.

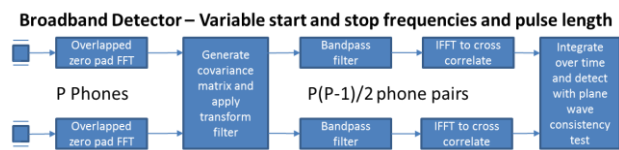


Fig. 15. High-level broadband detection processing string.

The zero padding on the FFT ensures that the correlation is not cyclical and must have a longer duration than the maximum travel time across the array, which is approximately 60µs for the blade sensor at endfire in a slow sound speed environment. Alternately, use of overlapped and windowed FFT allows the initial processing to be used for both narrowband and broadband detection with minimal degradation in the broadband case.

The cross spectral values generated from the FFTed phone data may be transformed in some manner in the general case to improve performance. This transform can be PHAT or SCOT or whatever the end user fancies.

The bandpass filters ensure only frequencies from an emitter of interest are used to generate the correlation function for each phone pair. Frequency bands can cover a set of all reasonable ranges, or some may be chosen based on emitters whose characteristics are known a priori.

An IFFT is then used to generate an interpolated cross-correlation function. In many cases, the cross-correlation function will have multiple strong peaks that are similar in magnitude in the TDoA range of -60µs to 60µs due to sparseness of the array at higher frequencies and insufficient signal bandwidth.

Finally, the correlation functions are integrated over time matching the pulse length being searched for and detection is usually established based on some form of consistency test. In the figure, a simple plane-wave test is used to establish that the incoming wave front is roughly a plane-wave from a far-field emitter.

The output parameters are the emitter's frequency range, duration and start time, along with an angle of arrival. The signal strength, smoothed coherence, and plane wave consistency are also available.

Broadband processing generally provides fewer and lower quality classification features relative to narrowband processing.

3.2 Performance

Limitations in counter-detection range at higher frequencies due to absorption loss are well known, but these ranges are still longer than most would assume. Absorption loss in seawater is a function of frequency, temperature, depth, salinity, and pH which is used to estimate the concentration of MgSO₄. Figure 16 below shows absorption loss at frequencies up to 1 MHz in dB per km in four major waterways. Significant differences are evident with the Baltic having much lower absorption losses between 2kHz and 200kHz and the Red Sea having much higher absorption losses from 70kHz to 400kHz.

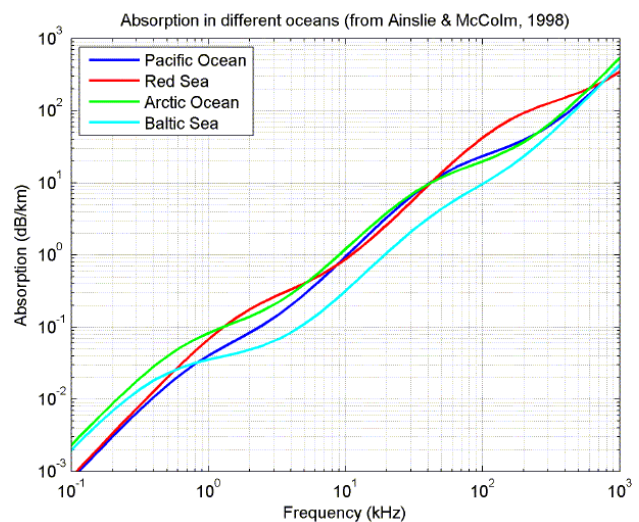


Fig. 16. Typical absorption loss in four waterways as a function of frequency at shallow depth from Ainslie & McColm, 1998.

Figure 17 shows TL (Transmission Loss) calculated as the sum of spreading loss and absorption loss as a function of range and frequency. Most high frequency sonars have SL (Source Level) above 185 dB re 1µPa per √Hz, so

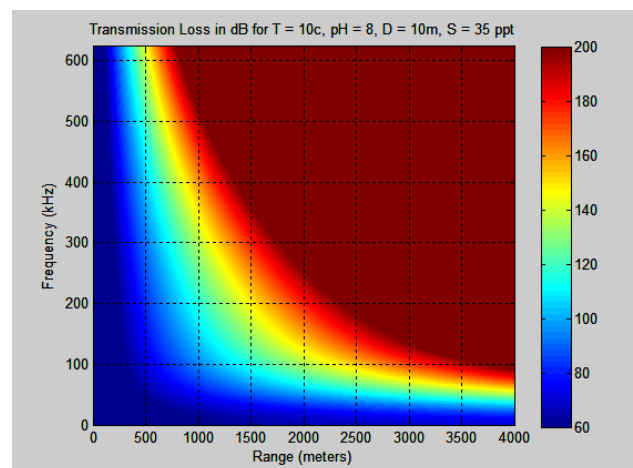


Fig. 17. TL (Transmission Loss) due to combined spreading and absorption as a function of range and frequency. Most high frequency broadband signals with TL of 140dB to 150dB will be readily detectable by a well-designed passive receiver.

probability of detection with TL of 140dB to 150dB should be high. This corresponds to the figure's yellow band. With a near optimal detector, counter-detection ranges greater than 2.3km are likely at frequencies below 100kHz, dropping to 1.5km at 200kHz, 1.1km at 300kHz, 900m at 400kHz, 700m at 500kHz and 500m at 625kHz.

4 Processing of tank test data

The potted unit was tank tested at Sensor Technology Ltd on a rotator shaft with frequencies between 10 kHz and 200 kHz, the high frequency tank's lower and upper limits. Data was recorded and frequency coverage and bearing estimation capability over this frequency range were demonstrated.

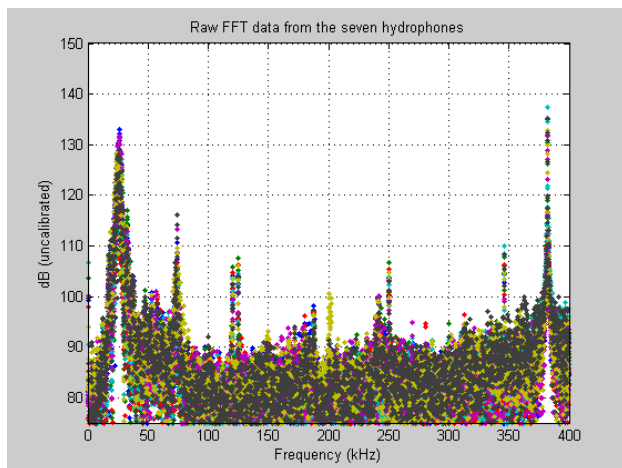


Fig. 18. 8K FFT data from the Blade Sensor during a 25 kHz pulse showing many narrowband and broadband noise sources.

Initial testing looked at the noise floor of the unit while it was mounted on the rotator shaft in Sensor Technology's test tank. This testing revealed many narrowband and broadband noise sources over the unit's wide frequency band as shown in figure 18 above. These noise sources may have the following sources:

- External noise sources
 - Acoustic noise in the test tank
 - Mechanical vibration from the rotator
 - Mechanical resonances of the rotator
 - EMI in the test tank room
- Self-noise sources
 - Mechanical resonances of the sensor
 - Mechanical noise from the input supply
 - Electrical noise from the input supply
 - Mechanical noise from the FPGA board
 - Electrical noise from the FPGA board
 - Electrical noise from the preamps
 - Electrical noise from the A/D converters

It was not possible during the short test period to isolate the noise sources, but the noise covariance was estimated for each FFT bin using a few seconds worth of data collected without a signal in the water, and testing showed that the noise covariance exhibits very high short-term stationarity. Noise sources that exhibit short-term

stationarity can be minimized using covariance processing if the noise covariance matrix can be accurately estimated.

Figure 19 below shows the FFT of the same hydrophone data as in figure 18 after noise covariance-based normalization.

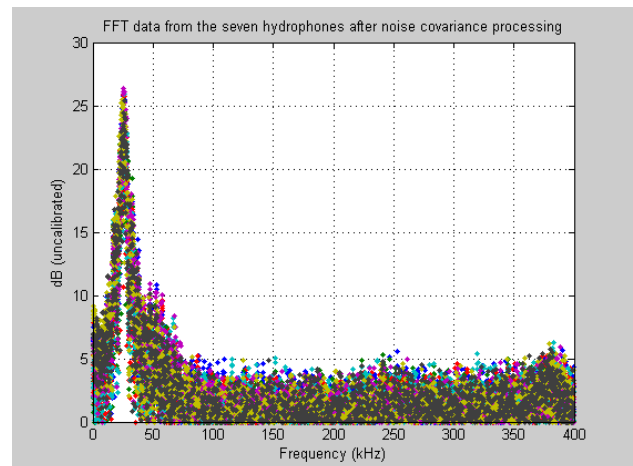


Fig. 19. The same data as the previous figure after noise covariance-based normalization.

The noise covariance can be used to provide detection as shown in figure 20 below. In this case, the phone inputs are being combined in a manner that minimizes noise variance rather than providing spatial gain. The strong signal at 25 kHz is approximately 90dB above the noise floor which is a very good result given the moderate level of the input signal. The bump at 380 kHz may be due to a switching power supply or it may be associated with the resonance frequency of the 1/2cm hydrophones.

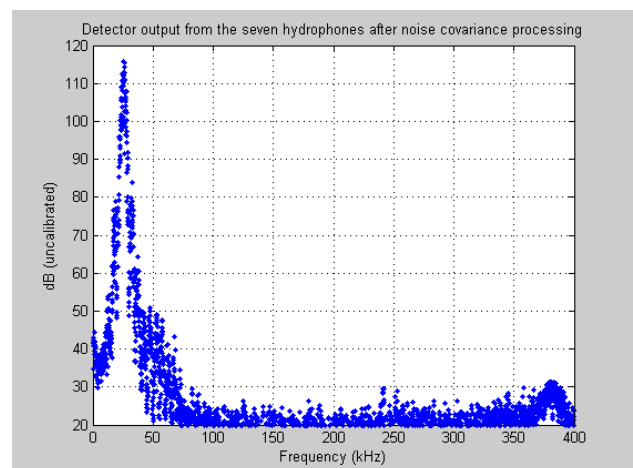


Fig. 20. A noise covariance-based detector which efficiently combines the hydrophone data to minimize noise variance rather than for beamforming.

After a detection is made, the TDoA (Time Delay of Arrival) data is generated for each pair of phones. This step is performed by bandpass filtering the FFTs, optionally performing a transform such as PHAT (Phase Transform), SCOT (Smoothed Coherence Transform) or SPED (Sub-band Peak Energy Detector) and taking the IFFT to obtain the interphone modified cross correlations. A peak of the correlation function should exist for each TDoA, but with

a sparse array there may be many peaks, and the correct peak is frequently not the peak with the highest magnitude.

An efficient plane wave test can be used to verify that the detection is coming from a far-field source and is likely to be valid. This test ensures that for each set of hydrophones, $\tau_{ij} + \tau_{jk} \approx \tau_{ik}$.

After determination that a detection is coming from a far field source, bearing is estimated by comparing the measured TDoA values for each hydrophone pair with measured values from many angles. This method is effective with accurate sound speed data near the array. Resulting bearing estimates at 25 kHz from early rotator shaft testing are shown in figure 21 below with the solid line giving ideal results.

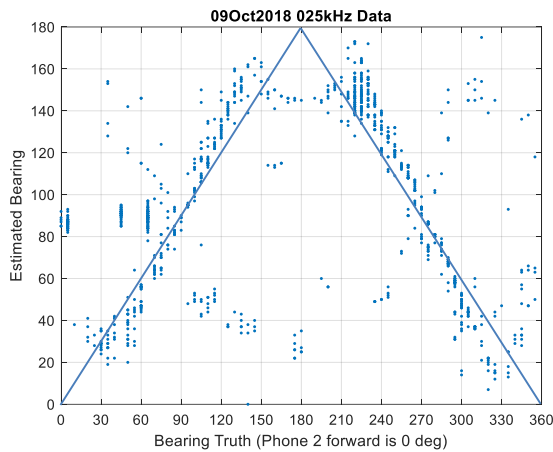


Fig. 21. Estimated bearing as a function of rotator shaft bearing where 90 and 270 degrees are at boresight. Solid lines show ideal results. Calculation is based on theoretical delays based on fresh water speed of sound.

Figure 22 below shows a plot of the RMS bearing accuracy associated with each detection. The bearing estimation was based on theoretical values for time delays in fresh water and is degraded by the high sound speed in

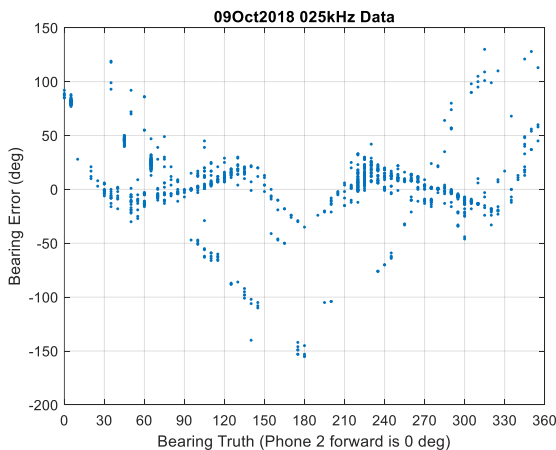


Fig. 22. RMS errors associated with the bearings above are shown based on bearing estimates based on theoretical delays. Reduced RMS errors can be obtained by associating angles with experimentally determined TDoA values. Calculations and plotting by D. Kershner at In-Depth Engineering.

the epoxy potting. More recent processing has produced results with significantly decreased RMS bearing errors.

Additional in-water testing will be performed in the coming months, including testing against a variety of active emitters at multiple ranges to provide data with varying SE (signal excess).

References

- [1] L3 Oceania, GPM 300 Acoustic Modem, <https://www2.l3t.com/oceania/pdfs/datasheets/GPM%20300%20Acoustic%20Modem.pdf>
- [2] Hydroid REMUS 100, Autonomous Underwater Vehicle, <https://www.km.kongsberg.com/ks/web/nokbg0240.nsf/AllWeb/D241A2C835DF40B0C12574AB003EA6AB?OpenDocument>

Author/Speaker Biographies

Alan T. Sassler is Extreme Sonar's Chief Scientist responsible for developing waveform generator, power amplifiers and receiver hardware for marine mammal detection and localization systems for the US Navy's surveillance ships. Mr. Sassler previously served as Director of Engineering at Advanced Acoustic Concepts and Chief Scientist at Analysis, Design & Diagnostics.